

Available online at [www.sciencedirect.com](http://www.sciencedirect.com)

Procedia Engineering 14 (2011) 552–558

---

---

**Procedia  
Engineering**

---

---

[www.elsevier.com/locate/procedia](http://www.elsevier.com/locate/procedia)

The Twelfth East Asia-Pacific Conference on Structural Engineering and Construction

# Use of Digital Surface Model Constructed from Digital Aerial Images to Detect Collapsed Buildings during Earthquake

Yoshihisa MARUYAMA<sup>a\*</sup>, Akira TASHIRO<sup>b</sup>, Fumio YAMAZAKI<sup>a</sup>

<sup>a</sup>Department of Urban Environment Systems, Chiba University, Chiba, Japan

<sup>b</sup>JR East Facility Management Co., Ltd., Japan (Former Student, Chiba University)

---

## Abstract

The collapsed buildings during the 2007 Niigata Chuetsu-oki earthquake are detected based on aerial photogrammetry using digital aerial images. The digital surface models in the area where severe damage incidents were observed after the earthquake are constructed using digital aerial camera images. The pre- and post-event aerial images are employed to obtain the digital surface models in this study. The differences of building heights between pre- and post-event models are considered to detect collapsed buildings and the accuracy of the method is discussed in this paper.

© 2011 Published by Elsevier Ltd. Open access under [CC BY-NC-ND license](https://creativecommons.org/licenses/by-nc-nd/4.0/).

*Keywords:* collapsed building, earthquake, digital aerial image, DSM, aerial photogrammetry.

---

## 1. INTRODUCTION

Remotely sensed data obtained from satellites and airborne platforms are useful in providing an understanding of the distribution of damage due to natural disasters (Yamazaki 2001). The platforms and sensors of remote sensing should be selected with regards to the coverage and resolution required and the urgency, weather and time conditions.

Recently, the digital aerial imaging system has become widely used (Hinz 1999; Leberl and Gruber 2005). The imaging system saves time associated with analog imagery processes and provides more precise and better-quality aerial images. In addition, the exterior orientations of airborne images can be

---

\* Corresponding author and presenter: Email: [ymaruyam@tu.chiba-u.ac.jp](mailto:ymaruyam@tu.chiba-u.ac.jp)

determined by integrating GPS (Global Positioning System) and IMU (Inertial Measurement Unit) observations made during the mapping flight. Hence, it is expected that the digital surface model (DSM) can be constructed with good accuracy using the images captured by the imaging system.

Aerial and satellite images are employed to detect collapsed buildings due to an earthquake. Mitomi et al. (2001) tried to reveal building debris automatically using images captured by a high-definition television camera. Saito et al. (2004) performed visual damage inspection using the post-event IKONOS image, in which individual buildings can be identified, and pre-event other satellite images for the 2001 Gujarat, India earthquake. QuickBird images with the maximum spatial resolution of 0.6 m were also employed to detect collapsed buildings after the 2003 Bam, Iran, earthquake (Yamazaki et al. 2005). The object-based classification technique using digital aerial images was applied to access damaged buildings in the 2007 Niigata Chuetsu-oki earthquake (Suzuki et al. 2010).

So far, remotely sensed images might be effective to detect earthquake induced damages. Since we can obtain only the top view of the affected area, some of the damaged buildings are difficult to reveal. Figure 1 shows an example of the aerial image captured after the 2007 Niigata Chuetsu-oki earthquake. A two-story building with the collapsed ground floor was found from the field photo. The building could not be pointed out from the aerial image because no damage was observed on its roof. This study employs the DSM constructed from the digital aerial images to reveal the differences of building heights between pre- and post-event models. Aerial photogrammetry is performed on the digital aerial images captured before and after the 2007 Niigata Chuetsu-oki earthquake in Kashiwazaki city, Niigata, Japan. The accuracy of this method is discussed comparing with the result of visual damage inspection.

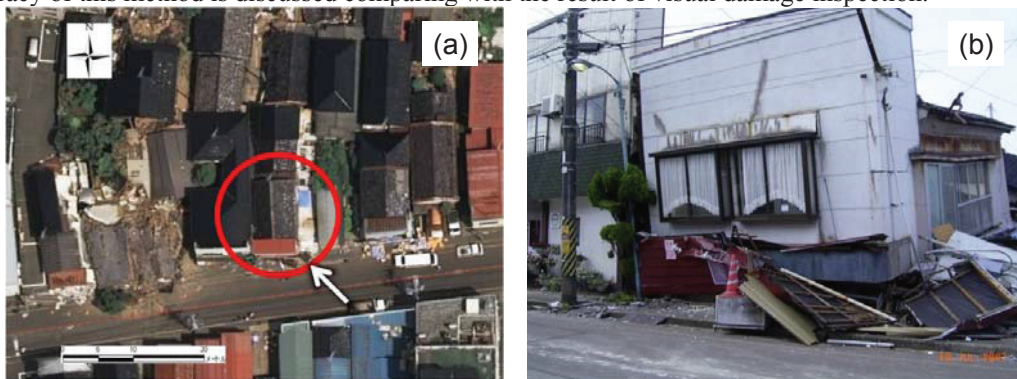


Figure 1: Comparison between (a) the aerial image and (b) the field photo of the two-story building with the collapsed ground floor after the 2007 Niigata Chuetsu-oki earthquake.

## 2. CONSTRUCTION OF THE 3D MODEL FOR BUILDINGS USING PRE-EVENT AERIAL IMAGE

The Niigata Chuetsu-oki earthquake occurred on July 16, 2007 with a JMA (Japan Meteorological Agency) magnitude of 6.8 (JMA, 2007). Severe ground shaking was observed near the epicenter and the JMA seismic intensity of 6+ was recorded in Kashiwazaki city, Niigata Prefecture, Japan. The number of collapsed buildings is 1,121 and that of casualties is 14 in the affected area.

The digital aerial image was captured for Kashiwazaki city on April 27, 2007, about three months before the earthquake. The digital aerial camera, UltraCamD, was employed to obtain the aerial images. The operated digital airborne imaging system was integrated with in-flight control systems consisting of

GPS and inertial measurement units (IMU). The altitude of aircraft during capturing was about 1970 m and the spatial resolution of the aerial images is about 0.17 m.

Performing aerial triangulation using the GPS/IMU dataset for the pre-event image with ground control points, the exterior orientations of airborne images can be determined accurately (Smith et al. 2005). The exterior orientations mean the three dimensional position and the three rotational angles of digital camera. The relative orientation of a stereo-pair of digital aerial images was conducted by introducing pass points, which are used as control points to match the two images, to reveal the accuracy of the exterior orientations. In this study, the exterior orientations of airborne images obtained from the aerial triangulation were employed to create stereo-pairs of digital aerial images.

Using a stereo-pair of aerial images, the two images were matched based on the image correlation method (Fua 1993). Then, the digital surface model (DSM) was constructed. Figure 2 shows the DSM obtained from the pre-event aerial images. In total, five sheets of aerial images were employed to obtain the DSM.

The DSM illustrated in Fig. 2 was constructed automatically after the creation of stereo-pairs of the aerial images. Due to the limitation of the automated method, the shape of buildings could not be extracted so accurately. Hence, the breaklines (Briese 2004), which describe the discontinuities of the elevations in 3D model, were developed from the pre-event DSM (Fig. 3). After the elevations were assigned to the both ends of breaklines, the 3D model for buildings were constructed based on the pre-event images (Fig. 4).

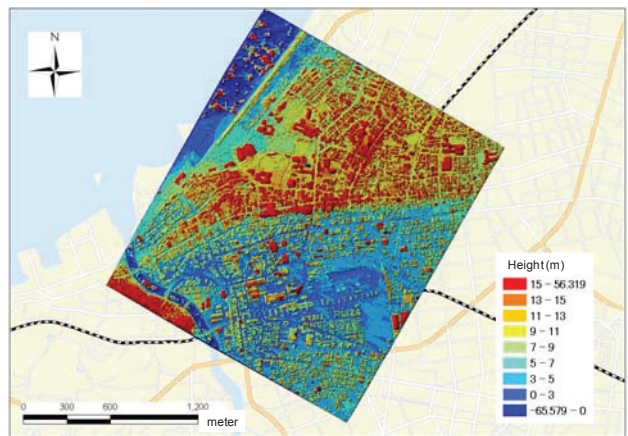


Figure 2: The digital surface model in Kashiwazaki city constructed from the pre-event images.

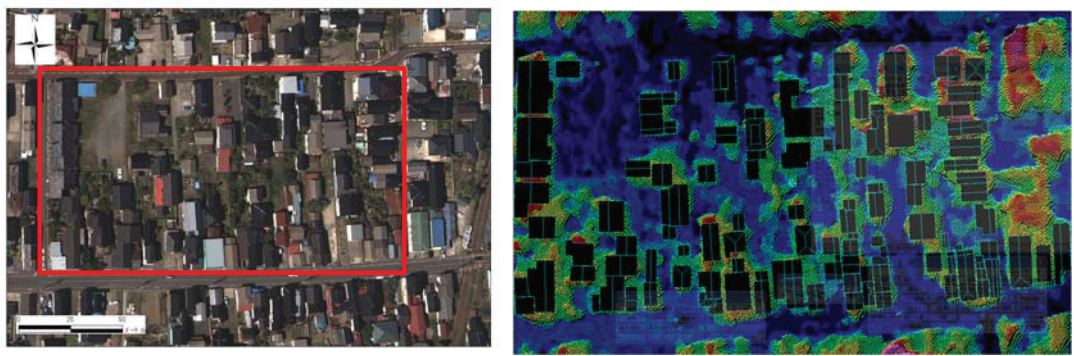


Figure 3: The digital surface model constructed automatically and the breaklines to describe the discontinuities of elevation.

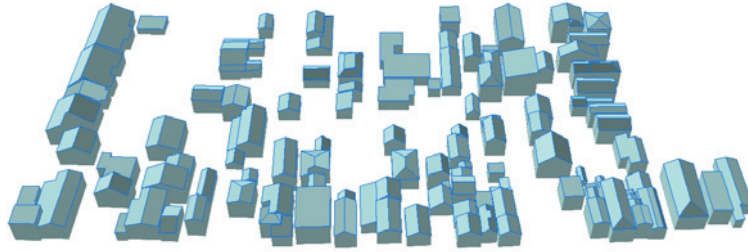


Figure 4: The 3D model for buildings constructed from the pre-event images.

### 3. DETECTION OF COLLAPSED BUILDINGS DUE TO THE NIIGATA CHUETSU-OKI EARTHQUAKE

#### 3.1. The DSM Constructed from the Post-event Aerial Images

As is shown in the previous chapter, the GPS/IMU system helps to determine the exterior orientations of airborne images and to save time to construct the DSM. The post-event digital aerial images were captured by Asia Air Survey Co., Ltd. on July 19, 2007 (three days after the earthquake). The digital mapping camera system (DMC) was employed to obtain the aerial images in the affected areas. The GPS/IMU system was also operated during the flight.

The GPS/IMU data of the post-event images was not adjusted with reference to the GPS-based control stations deployed by Geographical Survey Institute of Japan (GSI). GSI has established about 1,200 GPS-based control stations throughout Japan. The stations are not available for surveying after a damaging earthquake because of the effects of crustal movements. Although the DSM could be constructed automatically from the post-event images, the two DSMs from the pre- and post-event images could not be superposed. The DSM from the post-event images showed about 10 m less elevations and horizontal deformations.

To construct a proper DSM from the post-event images, some ground control points were extracted from the stereo-pairs of the pre-event images. Since the DSM from the pre-event images constructed accurately, the control points were used as references to determine the exterior orientations of the post-event images. Figure 5 shows examples of the control points extracted from the stereo-pair of the pre-event images. Totally, the 12 control points were extracted from the pre-event images.

The exterior orientations of the post-event images were calculated based on the locations of the 12 control points. Figure 6 shows the DSM of the post-event images, which were obtained automatically after the creation of stereo-pairs of the aerial images. Six sheets of the aerial images were employed to develop Fig. 6.





Figure 5: Extraction of control points from the stereo-pairs of pre-event images.

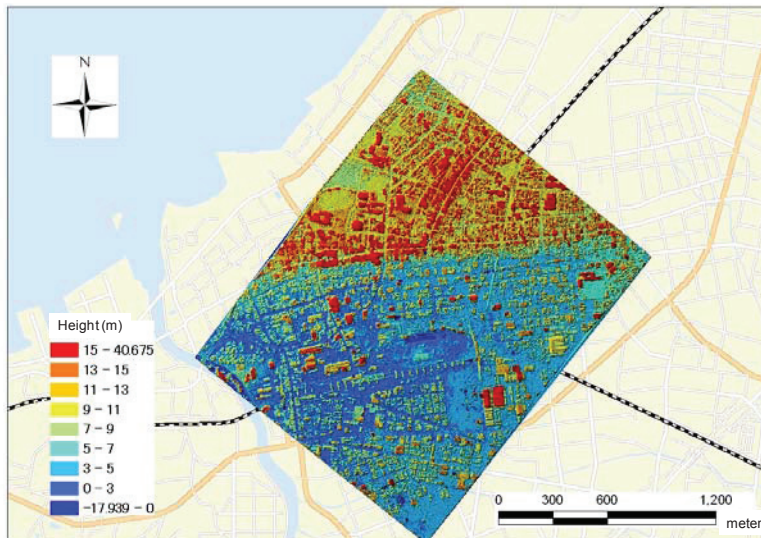


Figure 6: The DSM constructed from the post-event images.

### 3.2. Extraction of Collapsed Buildings

Based on the DSMs constructed from the pre- and post- event images, collapsed buildings due to the earthquake are extracted. The triangulated irregular network (TIN) was generated from the 3D model for the buildings shown in Fig. 4. Since the 3D model was constructed from the pre-event images considering breaklines, the heights of building are expected to produce rather accurate values.

As for the post-event images, immediacy was prioritized in this study. The DSM constructed automatically (Fig. 6) was used to detect collapsed buildings because it takes time to extract breaklines from the stereo-pair of aerial images. Subtracting the heights of the post-event DSM from those of the pre-event TIN, collapsed buildings were extracted. Figure 7(a) shows the results of this study. If the differences of the height between the pre- and post-event images were more than 2.5 m, the pixels were extracted as shown in red in Fig. 7(a).

The result of this study was compared with that of visual damage inspection (Fig. 7(b)). According to the visual inspection, there observed 19 totally or partially collapsed buildings and 90 non-damaged ones. The collapsed buildings were detected based on our proposed method. The non-damaged buildings were also recognized properly except for the right-upper part of the image where the post-event DSM contains much noise.

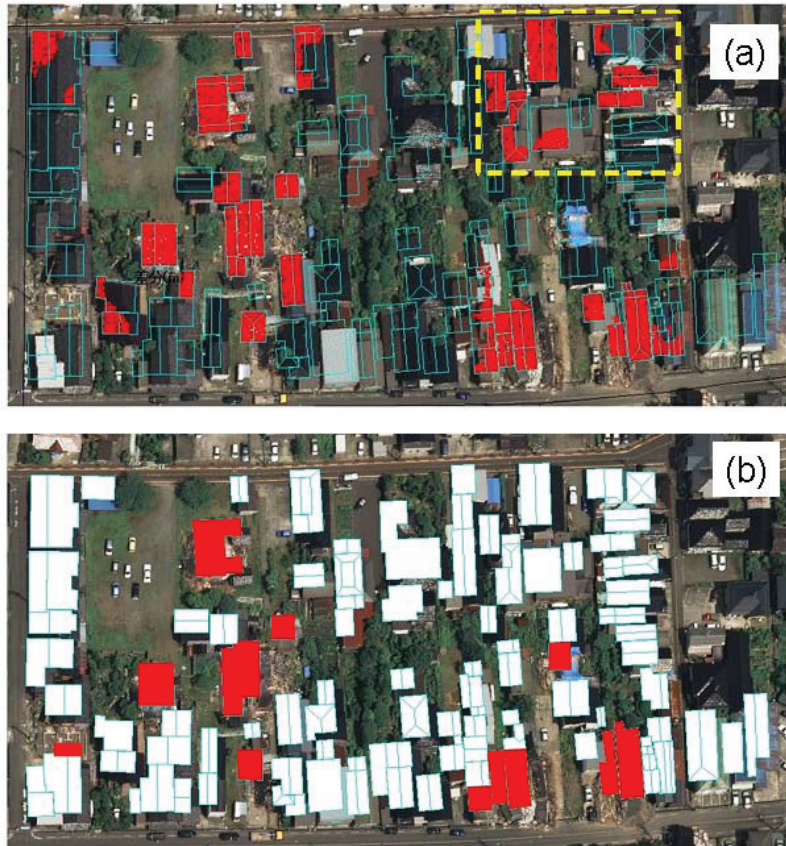


Figure 7: Detection of collapsed buildings based on (a) the pre- and post-event DSMs and (b) visual damage inspection.

#### 4. CONCLUSIONS

This study constructed digital surface models (DSMs) using aerial images captured by a digital airborne imaging system integrated with in-flight control systems consisting of GPS and inertial measurement units (IMU). Based on the constructed DSMs from the pre- and post-event images, the collapsed buildings due to the 2007 Niigata Chuetsu-oki earthquake were extracted.

After a damaging earthquake, the GPS-based control points are affected by crustal movements and they are difficult to be used for adjustment of GPS/IMU aviation data. Although the post-event DSM could be constructed automatically, it showed about 10 m less elevations and horizontal deformations comparing with the pre-event DSM. In order to modify the post-event DSM, the exterior orientations were calculated based on the locations of the 12 control points settled from stereo-pairs of the pre-event images.

Subtracting the heights of the post-event DSM from those of the pre-event one, the collapsed buildings were detected. The collapsed buildings were detected based on the proposed method. The non-damaged buildings were also recognized properly except for the area where the post-event DSM contains much noise.

**REFERENCES**

- [1] Briese C (2004). Three-dimensional modelling of breaklines from airborne laser scanner data. *International Archives of the Photogrammetry, Remote Sensing and Spatial Information Sciences*, 35(B3), pp. 1097-1102.
- [2] Fua P (1993). A parallel stereo algorithm that produces dense depth maps and preserves image features, *Machine Vision and Applications*, 6(1), pp. 35-49.
- [3] Hinz A (1999). The Z/I digital aerial camera system, *Proceedings of the 47th Photogrammetric Week 1999*, pp. 109-115.
- [4] Japan Meteorological Agency (2010). <http://www.seisvol.kishou.go.jp/eq/suikei/index.html>
- [5] Leberl F and Gruber M (2005). ULTRACAM-D: Understanding some Noteworthy Capabilities, *Proceedings of the 53th Photogrammetric Week 05*, pp. 57-68.
- [6] Mitomi H, Yamazaki F, and Matsuoka M (2001). Development of automated extraction method for building damage area based on maximum likelihood classifier. *Proceedings of the 8th International Conference on Structural Safety and Reliability*, CD-ROM, 8p.
- [7] Saito K, Spence R, Going C, and Markus M (2004). Using High-Resolution Satellite Images for Post-Earthquake Building Damage Assessment: A Study Following the 26 January 2001 Gujarat Earthquake. *Earthquake Spectra*, Vol. 20, No. 1, pp. 145-169.
- [8] Smith MJ, Qtaishat KS, Park DWG, and Jamieson A (2005). Initial results from the Vexcel UltraCam digital aerial camera. *Proceedings of ISPRS Hannover workshop 2005*, CD-ROM, 6p.
- [9] Suzuki D, Maruyama Y, and Yamazaki F (2010). Damage Detection of Wooden Houses after the Niigata-ken Chuetsu-oki Earthquake using Digital Aerial Images. *Journal of Japan Association for Earthquake Engineering*, Vol. 10, No. 3, pp. 33-45 (in Japanese).
- [10] Yamazaki, F (2001). Applications of remote sensing and GIS for damage assessment. *Proceedings of the 8th International Conference on Structural Safety and Reliability*, CD-ROM, 12p.
- [11] Yamazaki F, Yano Y, and Matsuoka M (2005). Visual Damage Interpretation of Buildings in Bam City Using QuickBird Images Following the 2003 Bam, Iran. *Earthquake, Earthquake Spectra*, Vol.21, No. S1, pp. S329-S336.